Maximum Sauter Mean Diameter and Terminal Velocity of Drops in a Liquid-liquid Spray Extraction Column

A. Salimi-Khorshidi[a], H. Abolghasemi[b,*], A. Khakpay[a], and N. Younes-Sinaki[a]

[a]Graduated in MSc of chemical engineering, School of Chemical Engineering, College of Engineering, University of Tehran
[b]Oil and Gas Center of Excellence, School of Chemical Engineering, College of Engineering, University of Tehran

The effect of holdup on Sauter mean drop diameter, d_{32} and the effect of d_{32} on terminal velocity have been investigated in a spray extraction column. There are two different zones for the dependence of d_{32} on holdup. d_{32} increased with an increase in holdup at low holdup levels and decreased with increasing holdup at high holdup levels. Variations in the terminal velocity of drops were similar to the dependence of d_{32} on holdup. Furthermore, empirical correlations have been derived to predict d_{32max} and terminal velocity and were in a good agreement with the experimental data. The derived correlations were compared with other researchers work and the results were in a satisfactory conformity.

Key words:
Mean drop diameter, holdup, spray column and terminal velocity

Introduction

Liquid-liquid extraction is a unit operation that is largely employed by process industries for separation purposes.[1] The liquid–liquid extraction columns are known as useful multiphase contacting equipment that received a wide industrial application in various fields of engineering such as hydrometallurgical, nuclear, petrochemical, pharmaceutical and food industries.[2–4]

Knowledge of predicting column drop size plays an important role in the processes of performance prediction and designing of spray column.[5–7] Large number of relatively stationary small drops will decrease the column capacity. Larger drops will have larger volume, low surface area per unit volume and higher slip velocity leading to the fact that the column height must be increased to achieve proper extraction efficiencies for such drops.[8–10] A large amount of work can be found in literature dedicated to the prediction of drop size distribution in liquid-liquid dispersions in extraction columns, but most of them are valid only for specific conditions of those studies.[11–16] Furthermore, maximum Sauter mean diameter, d_{32max}, has not been investigated yet in liquid-liquid extraction researches and hence, further research is needed in order to recognize this important parameter of every liquid-liquid emulsion system.

Another parameter which has great effect on the mass transfer coefficient in liquid-liquid emulsion systems is the terminal velocity.[17–19] Based on the study of the movement of a single drop of various sizes, Grace built his equation of terminal velocity. The terminal velocity equation that he proposed was:[20–21]

$$U_t = \frac{\mu_c}{d_{32}\rho_c}\left[\frac{g\mu_c^4\Delta\rho}{\rho_c^2\sigma^3}\right]^{-0.149}(J-0.857) \quad (1)$$

$$J = 0.94H^{0.757} \qquad 2 < H < 59.3 \quad (2)$$

$$J = 3.42H^{0.441} \qquad H \geq 59.3 \quad (3)$$

$$H = \frac{4}{3}Eo_d\left(\frac{g\mu_c^4\Delta\rho}{\rho_c^2\sigma^3}\right)^{-0.149}\left(\frac{\mu_c}{0.0009}\right)^{-0.14} \quad (4)$$

where U_t is the terminal velocity, d_{32} is Sauter mean diameter, ρ_c is the continuous phase density, μ_c is the continuous phase viscosity, $\Delta\rho$ is the density difference between two phases, g is the gravitational acceleration, and σ is the interfacial tension, and Eo_d is Eotvos number.

Eo_d was calculated from the following equation:

$$Eo_d = \frac{\Delta\rho g d_{32}^2}{\sigma} \quad (5)$$

*Corresponding Author: Hossein Abolghasemi, Associate Professor, School of Chemical Engineering, College of Engineering, University of Tehran, Enghelab Street, Tehran, Iran 11365/4563, Phone: 0098–21–66967791, E-mail: hoab@ut.ac.ir

There are other correlations derived by Petera et al. and Endres which are shown below, correspondingly.[22–23]

$$U_t = 0.249 d_{32} \left(\frac{g^2 \Delta \rho^2}{\rho_c \mu_c} \right) \qquad (6)$$

$$U_t = 1.23 \frac{\sigma}{\mu_c} \left(\frac{\sigma^3 \rho_c^2}{g \mu_c^4 \Delta \rho} \right) \qquad (7)$$

Prediction of d_{32max} occurrence point has an important role in investigating the extraction column performance. Because, at this point, the internal fluctuations of drops reach their highest level and as a result, the mass transfer coefficient will follow the same trend. In this study, d_{32} and the terminal velocity have been studied during the steady-state time-run for a spray extraction column. This paper presents measurement results of drop size and the terminal velocity in liquid-liquid emulsions in which three chemical systems (n-butanol-water-acetone, toluene-water-acetone and cumene-water-acetone) have been used. Furthermore, the effect of holdup on mean drop size and the effect of drop size on the terminal velocity have been studied and then, empirical correlations have been derived to be used for predicting maximum mean drop size and the terminal velocity.

Experimental

Apparatus

A glass column with a diameter of 10 cm and a length of 1.2 m was constructed with an interchangeable distributor positioned inside the column. Two similar digital pumps were used for pumping phases into the column. Moreover, three aluminous distributors with the nozzle diameters of 0.7, 1 and 1.3 mm were employed to produce drops. Fig. 1 shows a distributer used in the extraction column. Each distributor had 9 nozzle holes with a distance of 5 – 10 times the nozzle diameter between them. A digital camera (SONY, United Kingdom, DSC-F828 Model, 8 mega pixels resolution) was exploited to photograph the drops in order for measuring drops' size during experiments.

F i g . 1 – *Distributer of the extraction column*

Materials and methods

As mentioned above, three liquid-liquid systems were used in experiments. Toluene (purity>99 %, product of Merck Co., Germany, Lindenplatz), n-butanol (purity>99 %, product of Merck Co., Germany, Lindenplatz), and cumene (purity>99 %, product of Merck Co., Germany, Lindenplatz) were employed as dispersed phase and distilled water was used as continuous phase. Acetone (density = 791 kg m^{-3}, purity>99, viscosity 4×10^{-4} Pa s, product of Merck Co., Germany, Lindenplatz) has been utilized as the solute between two phases. The interfacial tension decreased slightly as the mass transfer occurred through the height of the column (by transportation of acetone). But, this decrease was ignorable (about 1 %). The liquid-liquid systems' properties are presented in Table 1.

The apparatus was washed carefully before each experiment to avoid the effect of pollutants on d_{32}. Furthermore, two phases had been saturated with each other to prevent the solubility effects.

Experiments began by pumping the continuous phase into the column. Having filled the column, pumping of the dispersed phase had commenced. Once reaching the steady state condition in the column, photographing of drops started. The drop size measurement was then carried out by analyzing recorded photos by means of AutoCAD 2004 software. More than 70 drops were analyzed for each experiment. A simple method was used to measure the size of photographed drops. Using this method, the size of drops was measured by comparing drops' size with a size-defined article, i.e. the column diameter, in each photo. The systematic parallax error

Ta b l e 1 – *Liquid-liquid systems' properties*

	ρ_c (kg m^{-3})	ρ_d (kg m^{-3})	μ_c (Pa s)	μ_d (Pa s)	σ (N m^{-1})
N-butanol-water-acetone	996	813	9.6×10^{-4}	2.3×10^{-3}	0.0017
Toluene-water-acetone	996	870	9.6×10^{-4}	5.7×10^{-4}	0.036
Cumene-water-acetone	996	866	9.6×10^{-4}	7.5×10^{-4}	0.0546

was avoided in our method by determining several reference points with a negligible error ($\approx \pm0.0001$). Therefore, the measured drop size was as closest as possible to the real drop size.

The drops could be in spherical, elliptical or other similar shapes, but in a specified mixture, the form of the drops was strongly connected to their size. Usually, with an increase in drop's size, the drop's shape altered from spherical to elliptical.[18] The area of the elliptical drop could be determined using the following equation:

$$A = \frac{\dot{A}}{2}\left[d_H{}^2 + \frac{d_V\,d_H}{E^2 - 1}\,ln\left(E + \sqrt{E^2 - 1}\right)\right] \quad (8)$$

$$E = \frac{d_H}{d_V} \quad (9)$$

where A is the drop area, E is the drop inertia, d_H is the horizontal diameter and d_V is the vertical diameter for non-uniform drops. A modified correlation to calculate the equal drop area (or equal diameter) is shown below as equation 10.

$$\frac{A}{A_e} = \frac{1}{2}\left[E^{2/3} + \frac{1}{E^{1/3}\sqrt{E^2 - 1}}\,ln\left(E + \sqrt{E^2 - 1}\right)\right] \quad (10)$$

where A_e is the equal drop area.

Finally, the equal drop diameter, d_e, was calculated by means of equation 11.

$$d_e = \sqrt{\frac{4A_e}{\pi}} \quad (11)$$

After measuring drops' size, the Sauter mean diameter was obtained via equation 12.

$$d_{32} = \frac{\sum N_i d_i^3}{\sum N_i d_i^2} \quad (12)$$

where N_i is the number of the drops with diameter d_i in a particular experiment.

The terminal velocity was calculated by measuring the average rising time of drops in experiments. Moreover, for measuring Holdup, Φ, samples were collected and the volume of each phase was determined. In order to achieve reliable results, the height of phases in the column was maintained constant. The holdup was calculated using the following formula:

$$\varphi = \frac{V_O}{V_O + V_W} \quad (13)$$

where V_O and V_W are the volumes of the organic and the aqueous phase, respectively.

In order to analyze d_{32max} and velocity, three series of experiments were carried out for each liquid-liquid system. Experiments were performed for each liquid-liquid system at three nozzle diameters (0.7, 1, and 1.3 mm), also at three and six different flow rates of dispersed phase (60, 70 and 80 mL min^{-1}) and continuous phase (100, 150, 200, 300, 400 and 500 mL min^{-1}), respectively. All 162 experiments were performed three times to test reproducibility and repeatability of experiments. The laboratory temperature was maintained at about 25 °C for all experiments.

Results and discussion

Effect of holdup on the mean drop size

Figs. 2, 3 and 4 show the effect of the holdup on d_{32} at three different flow rates of dispersed phase for three different nozzle diameters. For all liquid-liquid systems and nozzle diameters, with increasing holdup d_{32} increased until reaching a maximum after which d_{32} decreased (see Figs. 2, 3 and 4). It could be interpreted as a result of the fact that formation of the drops consisted of two stages. During the first stage, which is known as the dripping stage, the drop was stagnant and the dispersed phase was pumped into the drop causing the drop to be enlarged. At the second stage, recognized as the jetting stage, the formed drop departed from the distributor. The second stage took place as a result of conquering of buoyancy force to the interfacial tension and afterwards, the drop began to rise along the height of the column. In fact, the drop's neck was formed in the first stage (dripping stage) and then, the dispersed phase was injected into the drop. Increase in drop size continued as long as the interfacial tension force was larger than the buoyancy force on the drop. Consequently, the final volume of the drop could be calculated as the summation of the volume of the drop's neck and the volume of the injected dispersed phase. The volume of the injected dispersed phase was obtained by multiplying the rising time and the dispersed phase flow rate. By increasing the dispersed phase flow rate, the rising time decreased considerably and the effect of second stage on the drop size diminished significantly (up to the maximum drop size; see Figs. 2, 3 and 4). In addition, the volume of the injected dispersed phase decreased notably as a result of increasing dispersed phase flow rate. Moreover, by enlargement of drops, the buoyancy increased causing an earlier departure of drops from the distributor. As a result, drop size decreased. Furthermore, the drops distort to a jet of drops by further increasing the flow rate to high values (more than 120 mL min^{-1}). Generally, the jetting stage is more effective in the
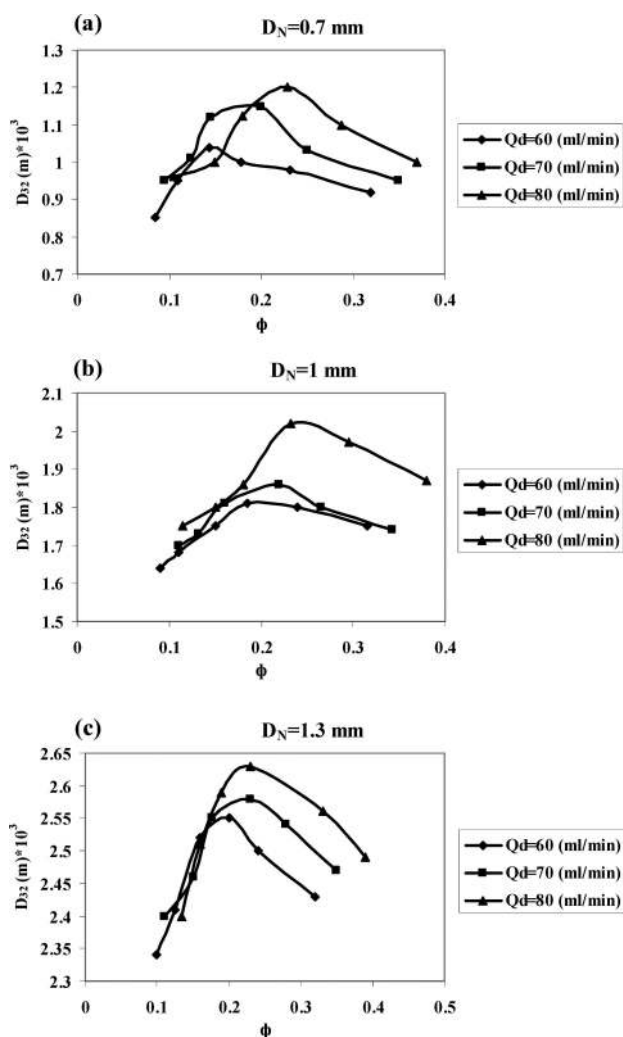
Fig. 2 – *Effect of the holdup on d_{32} for n-butanol-water-acetone system: (a) $Q_d = 60$ (mL min⁻¹); (b) $Q_d = 70$ (mL min⁻¹); (c) $Q_d = 80$ (mL min⁻¹)*

Fig. 3 – *Effect of the holdup on d_{32} for toluene-water-acetone system: (a) $Q_d = 60$ (mL min⁻¹); (b) $Q_d = 70$ (mL min⁻¹); (c) $Q_d = 80$ (mL min⁻¹)*

formation of drops, as the major part of drop's volume is formed during the jetting stage.

It was observed that d_{32} for the n-butanol-water-acetone system was the smallest in comparison with d_{32} of the other systems. Highest d_{32} belonged to the cumene-water-acetone system (see Figs. 2, 3 and 4). The difference between d_{32} of the systems was the consequence of the difference between their interfacial tensions as the cumene-water-acetone system and the n-butanol-water-acetone system had the highest and the lowest interfacial tension (and d_{32}), respectively.

There are two mechanisms for mass transfer: molecular diffusion and eddy diffusion (convection). In the rigid spheres, the mass transfers between two phases just by molecular diffusion, which is the result of concentration differences. However, at the bigger drops, convection and internal circulation are also effective parameters on the mass transfer. Furthermore, mass transfer is different for a drop in comparison with that of a group of drops.
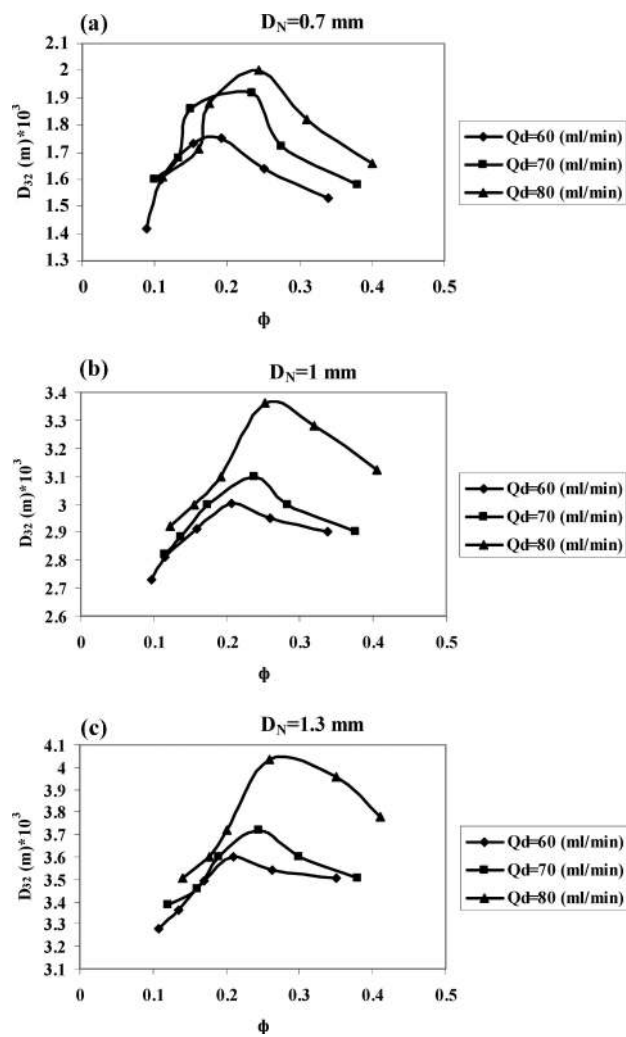
Effect of Sauter mean diameter on the terminal velocity

The effect of d_{32} on the terminal velocity at three different flow rates of dispersed phase for three different nozzle diameters are shown in Figs. 5, 6 and 7. For the n-butanol-water-acetone system, the terminal velocity increased with an increase in d_{32} until around 2.5 mm of d_{32}. After reaching a maximum known as the critical terminal velocity, the terminal velocity decreases. Moreover, the terminal velocity has not reached the critical terminal velocity in Figs. 5 (a) and (b), but Fig. 5 (c) shows the maximum terminal velocity for n-butanol-water-acetone system. It is clear from the Figures that the trend of curves is approximately similar for all liquid-liquid systems.

Furthermore, d_{32max} is about 3.1 for the toluene-water-acetone system and 3.5 mm for the cumene-water-acetone system. It can be due to the fact that the critical terminal velocity occurs when gravity and interfacial tension forces conquer buoy-
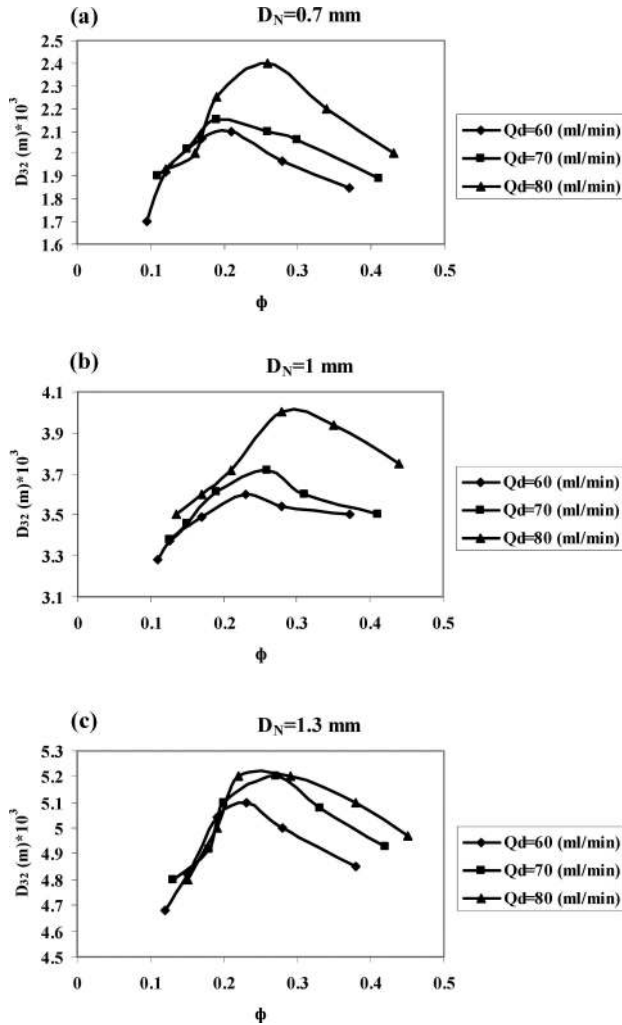
Fig. 4 – *Effect of the holdup on d_{32} for cumene-water-acetone system: (a) $Q_d = 60$ (mL min^{-1}); (b) $Q_d = 70$ (mL min^{-1}); (c) $Q_d = 80$ (mL min^{-1})*

ancy force of the drops. Subsequently, the enlargement of d_{32} leads to an increase in the internal fluctuations and rotations of the drops instead of an increase in terminal velocity. Therefore, the terminal velocity decreases. Moreover, the escalation of internal fluctuation of drops changes the shape of the drops from spherical to elliptical. Results showed that the n-butanol-water-acetone system was affected less than the toluene-water-acetone and cumene-water-acetone systems. Because, the n-butanol- water-acetone system had the smallest d_{32} in comparison with that of the other two systems and small drops behave like rigid spheres.

Modeling the maximum mean drop size

In order to model d_{32max}, a statistic analysis was carried out. All parameters which have an effect on d_{32max} are listed below as a function:

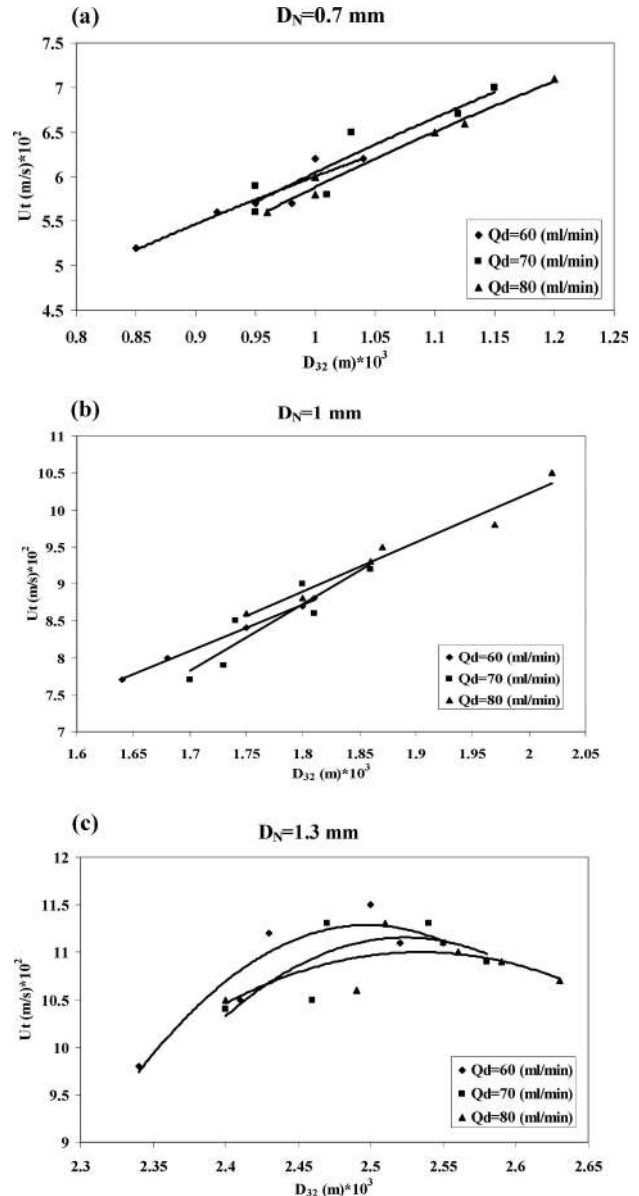Fig. 5 – *Effect of d_{32} on terminal velocity for n-butanol-water-acetone system: (a) $Q_d = 60$ (mL min^{-1}); (b) $Q_d = 70$ (mL min^{-1}); (c) $Q_d = 80$ (mL min^{-1})*

$$f\left(d_{32\,max}, \sigma, U_N, \rho_c, \rho_d, \Delta\rho, \mu_c, \mu_d, d_N, \varphi, g \right) = 0 \quad (14)$$

where U_N is the nozzle velocity, d_N is the nozzle diameter, and ρ_d is the dispersed phase density.

Equation (14) can be rephrased as the following equation, using dimensionless analysis:

$$f\left(\mathrm{Re}, We, \frac{d_{32}}{d_N}, \varphi \right) = 0 \quad (15)$$

where Re and We are Reynolds and Weber number, respectively.

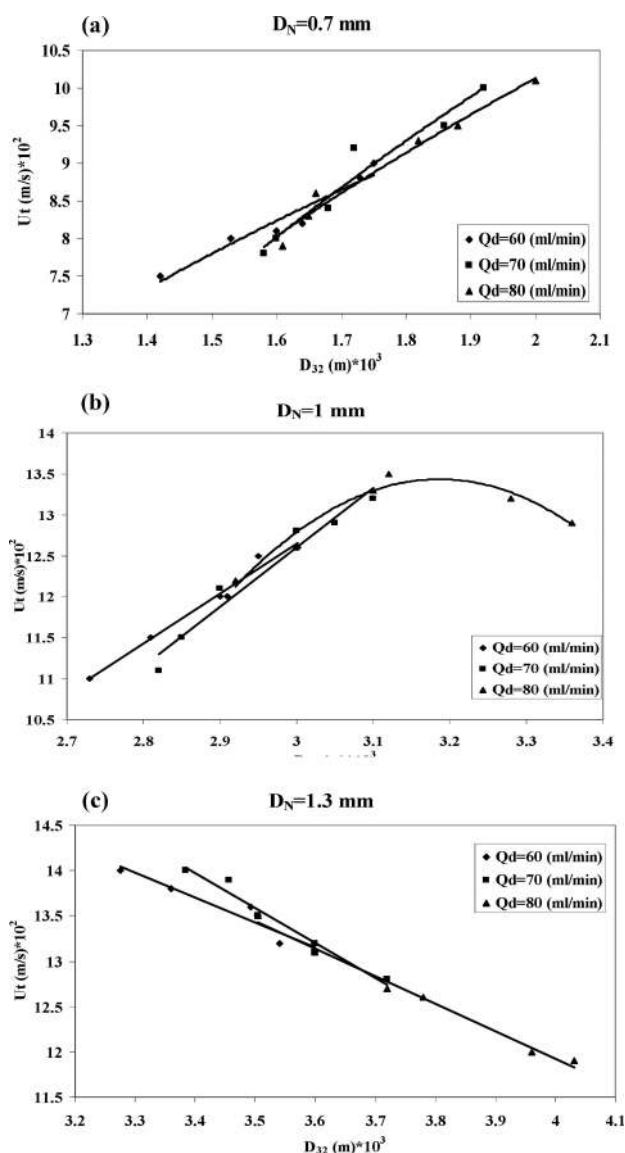Re and We can be determined by means of the following equations:

Fig. 6 – *Effect of d_{32} on terminal velocity for toluene-water-acetone system: (a) $Q_d = 60$ (mL min^{-1}); (b) $Q_d = 70$ (mL min^{-1}); (c) $Q_d = 80$ (mL min^{-1})*
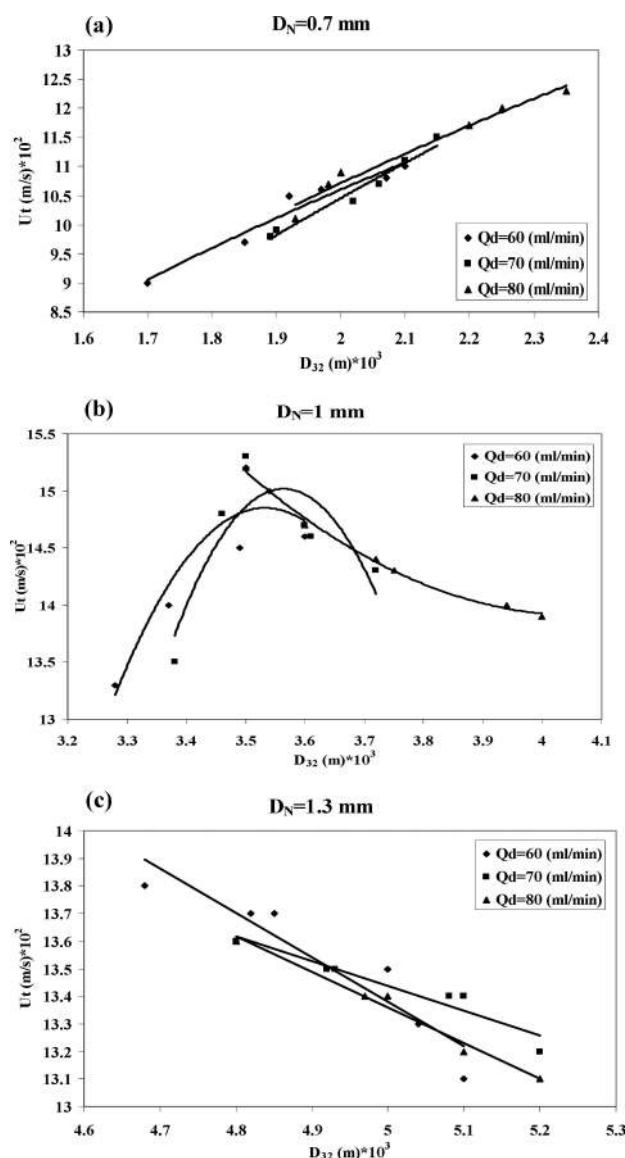

Fig. 7 – *Effect of d_{32} on terminal velocity for cumene-water-acetone system: (a) $Q_d = 60$ (mL min^{-1}); (b) $Q_d = 70$ (mL min^{-1}); (c) $Q_d = 80$ (mL min^{-1})*

$$Re = \frac{\rho_c U_N d_N}{\mu_c} \qquad (16)$$

$$We = \frac{\rho_c U_N^2 d_N}{\sigma} \qquad (17)$$

Equation (15) can be written in the form of the following equation:

$$\frac{d_{32\max}}{d_N} = a\varphi^b \, Re^m \, We^n \qquad (18)$$

where a, b, m and n are constants of the correlation.

Using the least squares method with the "Eviews" software, the correlation's constants were calculated[24]. In addition, the maximum points in

Figs. 2, 3 and 4 were used for calculations. Results are presented in Table 2.

According to Table 2, equation (19) can be proposed for predicting d$_{32\max}$:

$$\frac{d_{32\max}}{d_N} = 1.33\varphi^{0.51} \, Re^{0.31} \, We^{-0.16} \qquad (19)$$

The average absolute relative deviation, (%AARD) shown in Table 2 was calculated from the following equation:

Table 2 – *Calculation results for the constants of equation (20)*

Constants	a	b	m	n	%AARD	R-squared
Results	1.33	0.51	0.31	−0.16	5.64	0.93

$$\%AARD =$$

$$= \frac{1}{NE} \sum_{i=1}^{N} \left| \frac{(d_{32\max})_{\exp} - (d_{32\max})_{model}}{(d_{32\max})_{\exp}} \right| \times 100 \quad (20)$$

where NE is the number of experiments, $(d_{32\max})_{\exp}$ is the measured $d_{32\max}$ and $(d_{32\max})_{model}$ is the calculated $d_{32\max}$.

Fig. 8 displays a comparison between the calculated $d_{32\max}$ from equation (19) and the measured $d_{32\max}$ from experiments. It can be concluded from Fig. 8 that the correlations are in good agreement with the experimental data.
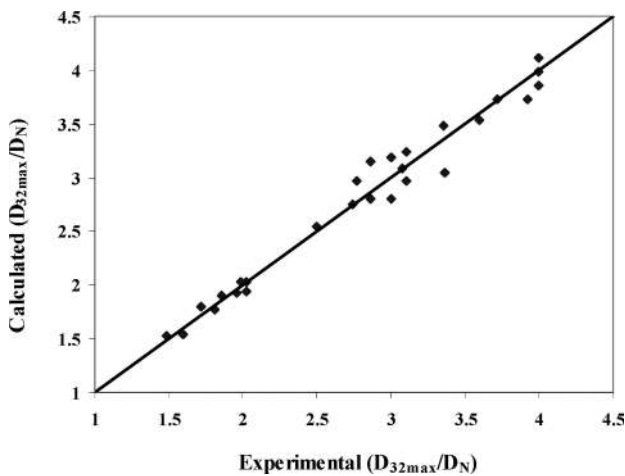

F i g . 8 – *Comparison of calculated and measured*

Modeling the terminal velocity

In order to take into account all phenomena that influence the terminal velocity, dimensionless numbers affecting the terminal velocity should be grouped. Therefore, equation (14) can be written, for terminal velocity, in form of equation (21):

$$f\left(\varphi, \mathrm{Re}, Eo, We, \frac{U_t}{U_N}, \frac{\mu_d}{\mu_c}, \frac{d_{32}}{d_N} \right) = 0 \quad (21)$$

where μ_d is dispersed phase viscosity and Eo is Eotvos number.

Eo can be calculated using the following equation:

$$Eo = \frac{\rho_c g D_N^2}{\sigma} \quad (22)$$

Equation (21) can be written in the form below:

$$\frac{U_t}{U_N} = a\varphi^b \, \mathrm{Re}^m \, Eo^n We^p \left(\frac{\mu_d}{\mu_c} \right)^q \left(\frac{d_{32}}{d_N} \right)^r \quad (23)$$

where a, b, m, n, p, q, and r are constants.

Constants of equation (23) were determined using least squares method with "Eviews" software.[24] The results are shown in Table 3.

According to Table 3, the correlation derived for predicting the terminal velocity (U_t) would be in the form of equation 24:

$$\frac{U_t}{U_N} = 2.92\varphi^{-0.01} \, \mathrm{Re}^{-0.23} \, Eo^{0.42} \cdot$$

$$\cdot We^{-0.42} \left(\frac{\mu_d}{\mu_c} \right)^{-0.10} \left(\frac{d_{32}}{d_N} \right)^{0.24} \quad (24)$$

A comparison between calculated U_t from equation (24) and measured U_t from the experiments is shown in Fig. 9. According to Fig. 9, the correlation demonstrates to be in a fine conformity with the experimental data.
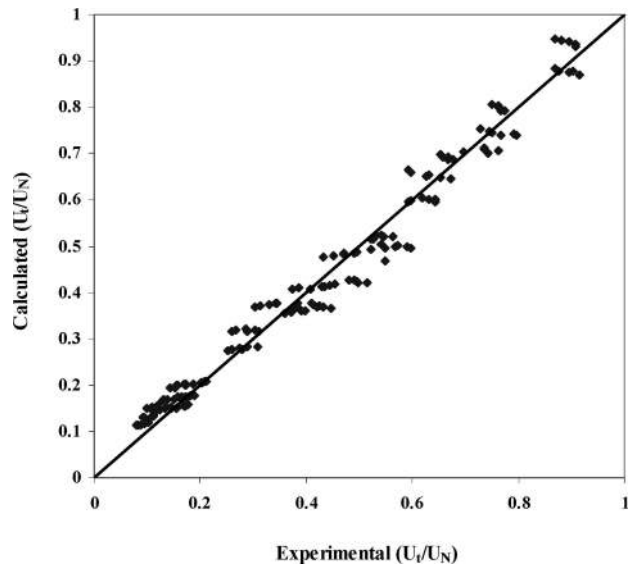

F i g . 9 – *Comparison of calculated and measured U_t*

To probe the accuracy of equation (24) and the results, equation (24) was compared with correlations of other researchers, i.e. Grace (equation 1), Petera (equation 6) and Endres (equation 7).[20–23] The results are shown in Table 4.

T a b l e 3 – *Calculation results for constants of equation (23)*

Constants	a	b	m	n	p	q	r	%AARD	R-squared
Results	2.92	−0.01	−0.23	0.42	−0.42	−0.10	0.24	10.81	0.98

Table 4 – *The comparison results of equation (24)*

	Grace's Model equation (1)	Petera's Model equation (6)	Endres's Model equation (7)
%AARD	30.27 %	34.02 %	24.34 %

In detail, the average deviation of equation (24) is about 30 %. These results show a good agreement between our experimental data and correlations of other researchers. Moreover, the correlation improved the error about 64 %.

Conclusions

An experimental investigation has been performed to evaluate the effect of holdup on d_{32} and the effect of d_{32} on the terminal velocity in a spray extraction column. Three liquid-liquid systems (n-butanol-water-acetone, toluene-water-acetone and cumene-water-acetone) have been used in the experiments. The results can be summarized as follows:

An increase in holdup had two distinct effects on mean drop size, d_{32}. At first, d_{32} increased with increasing holdup, but for holdup values exceeded a specific point, d_{32} lessened with an increase in holdup. Therefore, the d_{32}– holdup curve would have a maximum. In addition, smallest and largest d_{32} belonged to n-butanol-water-acetone system and cumene-water-acetone system, respectively.

The terminal velocity increased with intensification of d_{32}. After reaching a maximum, the terminal velocity declined with escalation of d_{32}. Moreover, the terminal velocity of n-butanol-water-acetone system was less sensitive to d_{32} growth in comparison with that of the other two systems.

For both d_{32max} and the terminal velocity, a new and modified empirical correlation was derived that agreed well with the experimental data. The average absolute relative deviation value was 5.64 % and 10.81 % for d_{32max} and the terminal velocity, respectively. Finally, a comparison between the derived correlation for terminal velocity (equation 24) and the other researchers' correlations showed a reasonable deviation of the derived correlation of this study from the mentioned correlations.[20–23]

Nomenclature

%AARD – Average absolute relative deviation

$(d_{32max})_{exp}$ – Measured maximum of d_{32} (m)

$(d_{32max})_{model}$ – Calculated maximum of d_{32} (m)

a   – Numerical coefficients in equations (20) and (24)

A   – Drop area (m^2)

A_e – Equal drop area (m^2)

b   – Numerical coefficients in equations (23) and (24)

d_{32} – Sauter mean diameter (m)

d_{32max} – Maximum Sauter mean diameter (m)

d_e – Equal drop diameter (m)

d_H – Horizontal diameter (m)

d_i – Diameter of class i (m)

d_N – Nozzle diameter (m)

d_V – Vertical diameter (m)

E   – Drop inertia

Eo   – Nozzle Eotvos number

Eo_d – d_{32} Eotvos number

g   – Gravitational acceleration (m s^{-2})

H   – Helping phrase equations (2), (3), and (4)

J   – Helping phrase equations (1), (2), and (3)

m   – Numerical coefficients in equations (20) and (24)

n   – Numerical coefficients in equations (20) and (24)

NE   – Number of experiments

N_i – Number of similar drops

p   – Numerical coefficients in equations (20) and (24)

q   – Numerical coefficients in equations (20) and (24)

Q_d – Dispersed phase flow rate (m^3 s^{-1})

r   – Numerical coefficients in equations (24)

Re   – Continuous phase Reynolds number

U_N – Nozzle velocity (m s^{-1})

U_t – Terminal velocity (m s^{-1})

V_O – Organic phase volume (m^3)

V_W – Aqueous phase volume (m^3)

We   – Weber number

Greek letters

μ_c – Continuous phase viscosity (Pa s)

μ_d – Dispersed phase viscosity (Pa s)

$\Delta\rho$ – Density difference between two phases (kg m^{-3})

ρ_c – Continuous phase density (kg m^{-3})

ρ_d – Dispersed phase density (kg m^{-3})

σ – Interfacial tension (N m^{-1})

Φ – Holdup

Subscripts

c   – Continuous phase

d   – Dispersed phase

References

1. *Menwer, M., Attarakih, Bart, H.O., Faqir, N.M.,* Chem. Eng. Sci. **61** (2006) 113.
2. *Saien, J., Daliri, S.,* Ind. Eng. Chem. Res. **47** (2008) 171.
3. *Saien, J., Daliri, S.,* Ind. Eng. Chem. Res. **48** (2009) 10008.
4. *Lohner, H., Czisch, C., Lehmann, P., Bauckhage, K.,* Chem. Eng. Technol. **24** (2001) 1157.
5. *Hashem, M.A.,* Alexandria Eng. J. **44 (3)** (2005) 477.

6. *Ceylan, S., Kelbaliyev, G., Ceylan, K.,* Colloids Surf., A **212** (2003) 285.

7. *Gabler, A., Wegener, M., Paschedag, A.R., Kraume, M.,* Chem. Eng. Sci. **61** (2006) 3018.

8. *Tcholakova, S., Denkov, N.D., Danner, N.,* Langmuir **20** (2004) 7444.

9. *Wegener, M., Grünig, J., Stüber, J., Paschedag, A.R., Kraume, M.,* Chem. Eng. Sci. **62** (2007) 2967.

10. *Chun, B.S., Wilkinson, G.T.,* Ind. Eng. Chem. Res. **39** (2000) 4673.

11. *Desnoyer, C., Masbernat, O., Gourdon, C.,* Chem. Eng. Sci. **58** (2003) 1353.

12. *Usman, M.R., Sattar, H., Hussain, S.N., Muhammad, H., Asghar, A., Afzal, W.,* Braz. J. Chem. Eng. **26** (2009) 677.

13. *Khakpay, A., Abolghasemi, H., Salimi-Khorshidi, A,* Chem. Eng. Process. **48 (6)** (2009) 1105.

14. *Khakpay, A., Abolghasemi, H., Montazer-Rahmati, M.M.,* Can. J. Chem. Eng. **88 (1)** (2010) 101.

15. *Salimi-Khorshidi, A, Abolghasemi, H., and Khakpay, A.,* 12th Iranian Chemical Engineering Congress, Tabriz, Iran (2008).

16. *Varfolomeev, B.G., Pebalk, V.L., Chigogidze, K.Sh., Lan, N.N., Fernando, R.S.,* Theor. Found. Chem. Eng. **34** (2000) 556.

17. *Perrut, M., Loutaty, R.,* Chem. Eng. J. **3 (3)** (1972) 286.

18. *Seibert, A.F., Fair, J.R.,* Ind. Eng. Chem. Res. **27** (1988) 470.

19. *Abolghasemi, H., Kheirjooy, Z., Salimi-Khorshidi, A, and Khakpay, A.,* 12th Iranian Chemical Engineering Congress, Tabriz, Iran (2008).

20. *Grace, J.R.,* Hydrodynamics of Liquid Drops in Immiscible Liquids, Chapter 38, Handbook of Fluids in Motion, pp. 1003–1025, N.P. Cheremisinoff and R. Cupta, Editors, Ann Arbor Science, The Butterfield Group, Ann Arbor, M I, (1983).

21. *Morales, C., Elman, H., Perez, A.,* Comput. Chem. Eng. **31** (2007) 1694.

22. *Petera, J., Weatherley, L.R,* Chem. Eng. Sci. **56** (2001) 4929.

23. *Endres, J.C.T.,* 8th Brazilian Congress of Phase Equilibrium and Fluid Properties for Chemical Process Design, Brazil (2000).

24. Quantitative Micro Software LLC., EViews 4 User's Guide, ISBN 1–880411–28–8, (2002).